Multi-spectral Palmprint Recognition with Deep Multi-view Representation Learning

Xiangyu Xu[1,2], Nuoya Xu[1], Huijie Li[1], and Qi Zhu[1,2(✉)]

[1] College of Computer Science and Technology,
Nanjing University of Aeronautics and Astronautics, Nanjing 211106, China
zhuqi@nuaa.edu.cn
[2] Collaborative Innovation Center of Novel Software Technology
and Industrialization, Nanjing 210093, China

Abstract. With the widespread application of biometrics in identification systems, palmprint recognition technology, as an emerging biometric technology, has received more and more attention in recent years. Palmprint recognition mainly focuses on image acquisition, preprocessing, feature selection and image matching. Feature extraction and matching are usually the most essential processes in palmprint recognition, and most of the research is based on feature selection and image matching, and many researchers use rich knowledge in machine learning and computer vision to solve these problems. In this paper, we propose a deep multi-view representation learning based multi-spectral palmprint fusion method, which uses deep neural networks to extract feature representation of multi-spectral palmprint images for palmprint classification. In this manner, the unique features of different spectral palmprint images can be used to learn a view-invariant representation of each palmprint. By using view-invariant representation, we can get better palmprint recognition performance than single modality. Experiments are performed on PolyU palmprint data set to validate the effectiveness of the proposed method.

Keywords: Person identification · Biometrics · Feature extraction · Multi-view learning · Palmprint recognition · Deep learning

1 Introduction

In realistic applications, palmprint as one of the important biological characteristics of the human body, has the characteristics of unique features, high stability, good safety and easy collection [1–3]. It is widely applied in biometric identification [4–6]. Compared to other biometric traits, such as fingerprint images, palmprint images have more rich features for individual recognition. Most palmprint recognition algorithms are based on the holistic and feature. Due to the wide application of image acquisition technology under multi-spectral, complementary information between different spectra can be well applied to classification, such as red, green, and other channels. According to a previous study of Zhang et al. [7], due to skin tissue's different ability to transmit light of different wavelengths, multi-spectral imaging technology can be applied to palmprint information collection, which can obtain more detailed feature information

X. B. Zhai et al. (Eds.): MLICOM 2019, LNICST 294, pp. 748–758, 2019.
https://doi.org/10.1007/978-3-030-32388-2_61

under different cortical layers. Multi-spectral palmprint recognition utilizes information obtained from different spectral wavelengths for personal identification. Since the vein is key part of the palmprint, multi-spectral features are necessary to improve the accuracy and robustness of palmprint recognition [8–12].

In many problems, we have to face multiple "views" of training data while most of the models can only handle two views [13]. The views here can also be multiple modalities, such as text and image, text and video, different spectral of image or different languages of text. As with this type of problem, multi-spectral palmprint recognition has also attracted people's attention. In this paper, we will focus on the difficulty in multi-spectral palmprint fusion classification.

Multi-spectral palmprint has aroused people's attention, many of them are focus on seeking a common space of two spectral [14, 15], it can also be treated as a multi-view representation problem, multi-view techniques learn a representation of data that captures the sources of variation common to all views [13]. Canonical correlation analysis [16] is also widely used in this field, which attempted to learn a projection of each view to maximize the correlation of the two views, the difference between the two views can be eliminated, and the public representation of the two views is obtained. As a classical common space learning method, CCA uses linear projection to learn a new subspace. However, the kernel function have successes in subspace learning [17], an improve method KCCA uses kernel function instead of linear method and makes better results. Now, deep learning is popular, Andrew et al. [18] propose deep CCA which greatly improved the performance of the original CCA with neural network. All of the existing methods are limited between two modalities (spectrums), to handle more than two views, many multi-view canonical correlation analysis method has been proposed [19, 20]. Like Deep Hyperalignment [21], we propose a DNN based multi-view representation learning method that use multiple networks for each modality to eliminate the difference between spectral.

In this paper the contributions are as follow. We apply deep neural networks to multi-spectral palmprint recognition problems, and the proposed method can process multiple modalities rather than two simultaneously. Using the information complementarity between different modalities, a discriminant feature representation can be generated. The proposed multi-modality palmprint recognition method has a good improvement compared to the single-mode palmprint recognition method.

2 Related Work

Canonical correlation analysis [16] has good performance in multi-view representation learning and its improvement to the nonlinear and multiple views, which will be described in this section.

2.1 Canonical Correlation Analysis (CCA)

Canonical correlation analysis (CCA) is a classic method that finds two linear projections that make two random vectors maximally correlated and is a fundamental multi-view learning technique. Given two input views, $X_1 \epsilon \mathbb{R}^{d_1}$ and $X_2 \epsilon \mathbb{R}^{d_2}$, with covariance matrices, $\sum_{11}$ and $\sum_{22}$, respectively, and cross-covariance matrix $\sum_{12}$, the objective function is to maximize the correlation between them:

$$\begin{aligned}\left(u_1^*, u_2^*\right) &= \operatorname{argmax}_{\mathrm{u}_1 \epsilon \mathbb{R}^{d_1}, \mathrm{u}_2 \epsilon \mathbb{R}^{d_2}} corr\left(u_1^T X_1, u_2^T X_2\right) \\ &= \operatorname{argmax}_{\mathrm{u}_1 \epsilon \mathbb{R}^{d_1}, \mathrm{u}_2 \epsilon \mathbb{R}^{d_2}} \frac{u_1^T \sum_{12} u_2}{\sqrt{u_1^T \sum_{11} u_1 u_2^T \sum_{22} u_2}}\end{aligned} \tag{1}$$

2.2 Deep Canonical Correlation Analysis (DCCA)

In [18], deep canonical correlation analysis has been proposed, it is an extension of CCA that addresses the first limitation by finding maximally linearly correlated of two vectors with two non-linear transformations. By passing two input views through multiple fully connected layers with activation function and performing CCA on the output layer, linear projection is transformed into nonlinear. Let us use $f_1(X_1)$ and $f_2(X_2)$ to represent the result of network output layer. The weights of the network, W_1 and W_2, are trained through standard backpropagation to maximize the CCA objective:

$$\left(u_1^*, u_2^*, W_1^*, W_2^*\right) = \operatorname{argmax} corr_{u_1, u_2}\left(u_1^T f_1(X_1), u_2^T f_2(X_2)\right) \tag{2}$$

2.3 DNN Feature Learning in Palmprint Recognition

In [23], Zhao et al. proposed the use of deep belief networks to deal with palmprint recognition problems and achieved good performance. First, the training data is used for top-down network training, and then the model parameters are adjusted to obtain more robust performance. Finally, the test sample can obtain the predicted label information by optimizing the parameters of the network.

As deep learning becomes more and more powerful, deep neural networks are increasingly used in extracting features [24]. Unlike other linear methods, the complexity of deep networks can extract deeper features of the sample space. Many multi-view methods based on deep learning have been proposed. [22], some approaches of them use neural networks with an objective similar to that of CCA to get a unified representation of all of the views under the assumption that the two views can share a common space.

3 The Proposed Algorithm

The proposed multi-view representation learning method is shown in Fig. 1. Multiple networks are federated to learn their respective nonlinear mappings to project corresponding views into a common space. All views of a sample are mapped into the new space, in which the distances are as close as possible. Moreover, the GCCA objectives are applied independently to the output layer, making the new representation discriminative. GCCA is another extension of CCA, which addresses the limitation on the number of views of the data. The same sample of different views will be highly correlated in the new subspace learned by the network.

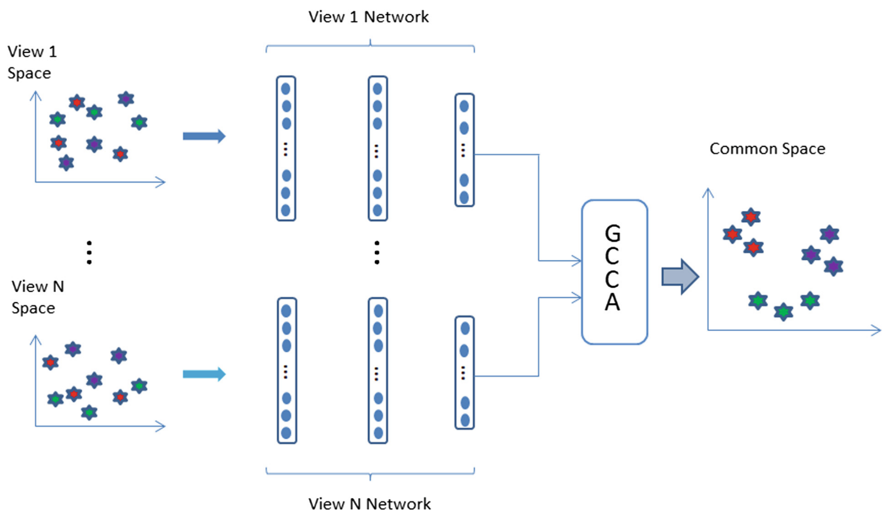

Fig. 1. The schematic of our proposed method for N views. Deep neural networks are jointly learned for each view, and GCCA uses its output for subspace learning. In the new space, all the views are maximally correlated. (The instance of same class is the same color) (Color figure online)

Multiple deep neural networks can learn common data representations from multiple views to eliminate differences of view. The network structure of our model refers to the DCCA network architecture which is simple full-connection layer architecture, and in the nonlinear part we use the sigmoid activation function. We train multiple nonlinear projections by updating the parameters of multiple networks by backpropagation to optimize the objective function, and then we use GCCA analysis to find the projection of each view, and use these projections as the fully connected layer of the last layer of the network. After training, Multi-view samples are nonlinearly mapped from high-dimensional space to a common low-dimensional space and then classified using sample features in low-dimensional space.

In order to learn the view-invariant representation from each view, we trained a network for each view. It is worth noting that the parameters and structure of the network of each perspective can be different from each other. This is specifically adjusted according to different problems. In the competition for multi-spectral palmprints, we have adopted the same network structure.

To this problem, the training set is denoted as $\mathcal{X} = \{(x_1^i, \ldots, x_V^i) | x_1^i \in X_1, \ldots, x_V^i \in X_N, 1 \leq i \leq N\}$, where $(x_1^i, \ldots, x_v^i)$ is a training data with V views and dimension is d. We try to find V nonlinear view-invariant transforms $f_v(x; \theta_v)$: $X_v \rightarrow Z_v$ that map the given data of multiple views to the common space Z_v. θ_v is the parameters of the v-th network.

In order to train a more robust classifier with discriminative representation, we need to make the same instance is close from different views using:

$$\min_U \sum\nolimits_{i=1}^{V} \sum\nolimits_{j=i+1}^{V} \left\| U_i^T Z_i - U_j^T Z_j \right\|_F^2 \text{ s.t. } U_i^T (Z_i Z_i^T) U_i = \mathrm{I} \;, i = 1 : V \tag{3}$$

From the model, nonlinear map of each view can be learned to maximize the correlation between the same samples across views. The network of v-th view consists of K_j layers, and k is at least four. For the v-th view, the output of the k-th layer is $h_k^v = s\left(W_k^v h_{k-1}^v + b_k^v\right)$, where $s : \mathbb{R} \to \mathbb{R}'$ is a nonlinear activation function and W_k^v and b_k^v is the weight matrix and bias matrix for k-th layer of the v-th view network. We denote the output of the final layer as Z_v.

Since Eq. (3) is calculated once for each new sample during the test phase, the calculation efficiency is not high. We rewrite Eq. (3) into the following form:

$$\min_{G,U} \sum\nolimits_{i=1}^{V} \left\|G - U_i^T Z_i\right\|_F^2 \text{ s.t. } G^T G = \mathrm{I} \tag{4}$$

where $\mathrm{G} \in \mathbb{R}^{r \times N}$ is the result of the projection of each view under ideal conditions.

Optimization: We utilize stochastic gradient descent (SGD) with mini-batches to solve this optimization problem.

It can be shown that the solution can be obtained by solving a certain eigenvalue problem. Define $C_{ii} = Z_i Z_i^T \in \mathbb{R}^{c_d^i \times c_d^i}$, and $U_i = C_{ii}^{-1} Z_i G^T$. Then the objective function can rewrite as follows:

$$\sum\nolimits_{i=1}^{V} \left\|G - U_i^T Z_i\right\|_F^2 = \sum\nolimits_{i=1}^{V} \left\|G - G Z_i^T C_{ii}^{-1} Z_i\right\|_F^2 \tag{5}$$

Since we define $\mathrm{M} = \sum_{i=1}^{V} P_i$, $P_i = Z_i^T C_{ii}^{-1} Z_i$, and the rows of G are the top r eigenvectors of M. Formula (5) can be rewritted as follow:

$$Jr - \mathrm{Tr}\left(GMG^T\right) \tag{6}$$

We can write the rank-1 decomposition of M as $\sum_{k=1}^{N} \lambda_k g_k g_k^T$. So g_k is the kth column of G, and the rows of Q are the N eigenvectors of M, then $\mathrm{Q}Q^T = I_N$.

$$\sum\nolimits_{k=1}^{N} \lambda_k g_k g_k^T = \sum\nolimits_{K=1}^{N} M g_k g_k^T = \mathrm{MG}G^T = M \tag{7}$$

since the matrix product $\mathrm{G}g_k = \hat{e}_k$,

$$\mathrm{GM}G^T = \sum\nolimits_{K=1}^{N} \lambda_k G g_k (G g_k)^{\mathrm{T}} = \sum\nolimits_{k=1}^{r} \lambda_k \hat{e}_k \hat{e}_k^{\mathrm{T}} \tag{8}$$

So, we can write the objective as

$$Jr - \sum\nolimits_{i=1}^{r} \lambda_i(M) \tag{9}$$

We denote the sum of eigenvalues $\sum_{i=1}^{r} \lambda_i(M)$ by L, by the chain rule, and using the fact that $\frac{\partial L}{\partial M} = G^T G$.

$$\frac{\partial L}{\partial (Z_i)_{ab}} = \sum\nolimits_{c,d=1}^{N} \frac{\partial L}{\partial M_{cd}} \frac{\partial M_{cd}}{\partial (Z_i)_{ab}} \tag{10}$$

Since $\mathrm{M} = \sum_{i=1}^{J} P_j$, $\frac{\partial M}{\partial Z_i} = \frac{\partial P_i}{\partial Z_i}$.

$$(P_i)_{cd} = \sum_{k,l=1}^{c_k^j} (Z_i)_{kc} \left(C_{ii}^{-1}\right)_{kl} (Z_i)_{ld} \tag{11}$$

In summary, Eq. (10) can be calculated as follows:

$$\frac{\partial L}{\partial (Z_i)_{ab}} = \sum_{c,d=1}^{N} \left(G^T G\right)_{cd} (I_N - P_i)_{cb} \left(C_{ii}^{-1} Z_i\right)_{ad} + \sum_{c,d=1}^{N} \left(G^T G\right)_{cd} (I_N - P_i)_{db} \left(C_{ii}^{-1} Z_i\right)_{ac} \tag{12}$$

After simplification we get the following results:

$$\frac{\partial L}{\partial (Z_i)_{ab}} = 2\left[C_{ii}^{-1} Z_i G^T G (I_N - P_i)\right]_{ab} \tag{13}$$

Therefore, since $U_i = C_{ii}^{-1} Z_i G^T$, the gradient of the objective function as follows:

$$\frac{\partial L}{\partial Z_i} = 2C_{ii}^{-1} Z_i G^T G (I_N - P_i) = 2U_i G - 2U_i U_i^T Z_i \tag{14}$$

Algorithm 1 illustrates the execution process of the proposed method.

Algorithm 1. Deep Multi-View Representation Learning

Input: multi-view data: $X_1, X_2, \ldots, X_J$,

number of iterations T, learning rate η

Output: $Z_1, Z_2, \ldots, Z_J$

1: Initialize neural network parameter $\theta_1, \theta_2, \ldots, \theta_J$

2: **for** iteration $t = 1,2,\ldots,T$ **do**

3: **for** each view $j = 1,2 \ldots, J$ **do**

4: $Z_j \leftarrow$ forward pass of X_j with network parameter θ_j

5: mean-center Z_j

6: **end for**

7: $U_1, \ldots, U_J, G \leftarrow gcca(Z_1, \ldots, Z_J)$

8: **for** each modality $j = 1,2 \ldots, J$ **do**

9: $\partial F / \partial Z_j \leftarrow U_j U_j^T Z_j - U_j G$

10: $\nabla\theta_j \leftarrow \mathrm{backprop}(\partial F / \partial Z_j, \theta_j)$

11: $\theta_j \leftarrow \theta_j - \eta \nabla\theta_j$

12: **end for**

13: **end for**

14: **for** each modality $j = 1,2 \ldots, J$ **do**

15: $Z_j \leftarrow$ forward pass of X_j with weights W_j

16: mean-center Z_j

17: **end for**

18: $U_1, \ldots, U_J, G \leftarrow gcca(Z_1, \ldots, Z_J)$

19: **for** each modality $j = 1,2 \ldots, J$ **do**

20: $Z_j \leftarrow U_j^T Z_j$

21: **end for**

4 Experiment

4.1 Palmprint Database

In this paper the database we used to verify the proposed method is the PolyU multispectral palmprint Database. The multispectral palmprint images of the database were collected from 250 volunteers, they are between the ages of 20 and 60, and the ratio of male to female is about four to one. The samples were collected twice, each time collecting 6 samples, and the two collections were separated by 9 days. Therefore, each person collects a total of 24 palm pictures including the left and right hands. The multispectral palmprint dataset is acquired under the red, green, blue, and near infrared (NIR) illuminations. In total, the database contains 6,000 images from 500 different palms for each illumination. We can treat each illumination as a view of sample, and more unique representation of palmprint image can be obtained. In Fig. 2, we show four typical regions of interested (ROI) images from different illuminations of the PolyU database. In the experiment, the six images of each palm are divided into the training sets and the other six are divided into testing sets.

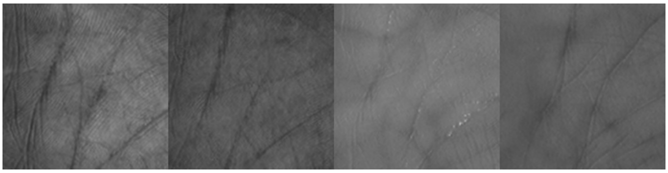

Fig. 2. Four palmprint samples selected from the PolyU _Red, PolyU _Green, PolyU _Blue, and PolyU _NIR palmprint databases.

4.2 Single Modality Palmprint Identification

The accuracy of the four spectral palmprints on the three baseline methods is listed in Table 1. Support Vector Machine is a classic supervised learning method with associated learning algorithms that analyzes data used for classification and regression analysis. k-nearest neighbors algorithm (k-NN) is a non-parametric method used for classification and regression. The idea of k-NN is that if the k samples most similar to a certain sample belong to a certain category in the feature space, the samples also belongs to this category. Deep belief network (DBN) is a classical deep neural network to be further trained with supervision to perform classification.

Table 1. Accuracy (%) of four spectral palmprints on baseline methods.

	SVM	k-NN	DBN
Red	92.93	96.86	71.63
NIR	89.76	95.56	63.4
Green	92.23	95.83	68.43
Blue	93.06	96.76	69.5

4.3 Multi-modality Palmprint Identification

In multi-modality palmprint verification experiments, we combined the four modality palmprint data in a total of five combinations: BDI, BGR, BIR, GIR, and BGIR. Randomly select six images of each palm as training data, and the remaining images as test data. In order to verify the effectiveness of our method, we chose some state-of-the-art methods as comparative methods including PCA, LDA, competitive code, LOBP, half orientation, MCCA, MKI, MvDA. Principal component analysis (PCA) and linear discriminant analysis (LDA) are the popular dimensionality reduction methods, the former one is supervised and the latter is unsupervised. Competitive coding extracts information from the palm line using Gabor filters, then use the matching algorithm to match the two sets of codes [25]. Local Orientation Binary Pattern (LOBP) method mainly captures the direction relationship information between the center point and the neighboring point, and then filters the local information into the final global information [26]. Half-orientation extraction method defines a bank of "Half-Gabor" filters for palmprint matching [27]. The three methods abovementioned are popular palmprint recognition method based on coding. Multi-view CCA(MCCA) [19] is an expansion of Linear CCA, it can handle multi-view problems. Multi-kernel learning method (MKL) is a common multi-view model, which use multiple kernel function to find the projection to high kernel space. Multi-view discriminant analysis (MvDA) jointly learns multiple view-specific linear projections to project multiple views into a common subspace. The recognition results are presented in Table 2.

Table 2. ACC (%) of different methods on PolyU palmprint databases.

Methods	PCA	LDA	Competitive code	LOBP	Half orientation	MCCA	MKl	MvDA	Ours
BGI	96.67	95.23	96.60	98.89	96.74	94.36	97.33	98.12	**99.45**
BGR	97.76	97.40	96.67	98.89	96.79	95.61	98.40	97.00	**99.63**
BIR	98.40	97.10	96.47	98.91	96.38	96.90	97.83	99.00	**99.42**
GIR	98.40	96.96	96.41	98.91	96.44	97.10	98.40	95.40	**99.37**
BGIR	98.40	98.46	96.58	98.90	96.68	96.29	98.40	96.97	**99.65**

The receiver operating characteristic (ROC) curve is adopted to further evaluate the effectiveness of the proposed method, which is a graph of genuine accept rate (GAR) versus false accepted rate (FAR) on all possible decision thresholds. Figure 3 is the ROC curves of the proposed method and three popular methods.

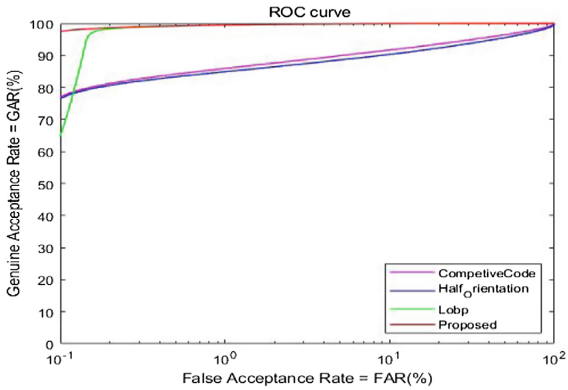

Fig. 3. The ROC curve of the proposed and other comparison method.

In addition, the equal error rate (EER), which is the point of false accept rate when it equals to false reject rate, is calculated as the basis of the evaluation. The EERs obtained using different methods are listed in Table 3.

Table 3. EERS of different methods.

Methods	Competitive code	LOBP	Half orientation	Proposed
BGI	0.0832	0.0780	0.0882	0.0712
BGR	0.0869	0.0750	0.1019	0.0722
BIR	0.0832	0.0790	0.0920	0.0753
GIR	0.0816	0.0800	0.0928	0.0736
BGIR	0.0922	0.0700	0.0893	0.0612

5 Conclusion

In this paper, we combine the unique characteristics of images under different illumination to solve the problem of multi-spectral palmprint recognition. We use deep neural networks to convert multispectral palmprint data into a common space where the distance of the same type of palmprint data is as small as possible. In the new space obtained, the palmprint can be better classified. A series of experimental results on polyU's multi-spectral palmprint dataset show that our proposed method has good performance on multi-spectral palmprint recognition. In the future work, we will optimize the efficiency and architecture of the model and explore the potential of this method in other palmprint recognition problems.

Acknowledgments. This work was supported in part by National Natural Science Foundation of China (Nos. 61501230, 61732006, 61876082 and 81771444), National Science and Technology Major Project (No. 2018ZX10201002), and the Fundamental Research Funds for the Central Universities No. NJ2019010.

References

1. Zheng, Q., Kumar, A., Pan, G.: Suspecting less and doing better: new insights on palmprint identification for faster and more accurate matching. IEEE Trans. Inf. Forensics Secur. **2**(5), 633–641 (2015)
2. Chakraborty, S., Bhattacharya, I., Chatterjee, A.: A palmprint based biometric authentication system using dual tree complex wavelet transform. Measurement **46**(10), 4179–4188 (2013)
3. Fei, L., Lu, G., Jia, W., Teng, S., Zhang, D.: Feature extraction methods for palmprint recognition: a survey and evaluation. IEEE Trans. Syst. Man Cybern.: Syst. **49**(2), 346–363 (2018)
4. Zhang, D.: Automated Biometrics: Technologies and Systems. Springer, New York (2013)
5. Jain, A., Ross, A., Prabhakar, S.: An introduction to biometric recognition. IEEE Trans. Circuits Syst. Video Technol. **14**(1), 4–20 (2004)
6. Chen, F., Huang, X., Zhou, J.: Hierarchical minutiae matching for fingerprint and palmprint identification. IEEE Trans. Image Process. **22**(12), 4964–4971 (2013)
7. Zhang, D., Kong, W., You, J., Wong, M.: Online palmprint identification. IEEE Trans. Pattern Anal. Mach. Intell. **25**(9), 1041–1050 (2003)
8. Han, D., Guo, Z., Zhang, D.: Multispectral palmprint recognition using wavelet-based image fusion. In: 9th International Conference on Signal Processing, pp. 2074–2077. IEEE (2008)
9. Hong, D., Liu, W., Su, J., Pan, Z., Wang, G.: A novel hierarchical approach for multispectral palmprint recognition. Neurocomputing **151**, 511–521 (2015)
10. Guo, Z., Zhang, L., Zhang, D.: Feature band selection for multispectral palmprint recognition. In: 20th International Conference on Pattern Recognition, pp. 1136–1139. IEEE (2010)
11. Hao, Y., Sun, Z., Tan, T., Ren, C.: Multispectral palm image fusion for accurate contact-free palmprint recognition. In: 15th IEEE International Conference on Image Processing, pp. 281–284. IEEE (2008)
12. Kisku, D., Rattani, A., Gupta, P., Sing, J., Hwang, C.: Human identity verification using multispectral palmprint fusion. J. Signal Inf. Process. **3**(2), 263 (2012)
13. Kan, M., Shan, S., Zhang, H., Lao, S., Chen, X.: Multi-view discriminant analysis. IEEE Trans. Pattern Anal. Mach. Intell. **38**(1), 188–194 (2015)
14. Yang, X., Sun, D.: Feature-level fusion of palmprint and palm vein base on canonical correlation analysis. In: 13th International Conference on Signal Processing (ICSP), pp. 1353–1356. IEEE (2010)
15. Li, M., Xie, W., Shen, L.: Fusing 3D gabor and block-wise spatial features for hyperspectral palmprint recognition. In: Zhou, J., et al. (eds.) CCBR 2017. LNCS, vol. 10568, pp. 361–369. Springer, Cham (2017). https://doi.org/10.1007/978-3-319-69923-3_39
16. Thompson, B.: Canonical correlation analysis. In: Encyclopedia of Statistics in Behavioral Science (2016)
17. Akaho, S.: A kernel method for canonical correlation analysis. arXiv preprint (2006)
18. Andrew, G., Arora, R., Bilmes, J., Livescu, K.: Deep canonical correlation analysis. In: International conference on machine learning, pp. 1247–1255 (2010)
19. Rupnik, J., Shawe-Taylor, J.: Multi-view canonical correlation analysis. In: Conference on Data Mining and Data Warehouses (SiKDD) (2010)
20. Benton, A., Khayrallah, H., Gujral, B., Reisinger, D., Zhang, S., Arora, R.: Deep generalized canonical correlation analysis. arXiv preprint arXiv:1702.02519 (2017)
21. Yousefnezhad, M., Zhang, D.: Deep hyperalignment. In: Advances in Neural Information Processing Systems, pp. 1604–1612 (2017)

22. Wang, W., Arora, R., Livescu, K., Bilmes, J.: On deep multi-view representation learning. In: International Conference on Machine Learning, pp. 1083–1092 (2015)
23. Xin, Z., Xin, P., Xiaoling, L., Xiaojing, G.: Palmprint recognition based on deep learning. In: IET (2015)
24. Minaee, S., Wang, Y: Palmprint recognition using deep scattering convolutional network. arXiv preprint arXiv:1603.09027 (2016)
25. Kong, A., Zhang, D.: Competitive coding scheme for palmprint verification. In: Proceedings of the 17th International Conference on Pattern Recognition, pp. 520–523. IEEE (2010)
26. Fei, L., Xu, Y., Teng, S., Zhang, W., Tang, W., Fang, X.: Local orientation binary pattern with use for palmprint recognition. In: Zhou, J., et al. (eds.) CCBR 2017. LNCS, vol. 10568, pp. 213–220. Springer, Cham (2017). https://doi.org/10.1007/978-3-319-69923-3_23
27. Fei, L., Xu, Y., Zhang, D.: Half-orientation extraction of palmprint features. Pattern Recogn. Lett. **69**, 35–41 (2016)